SCKs as nanoparticle carriers of doxorubicin: investigation of core composition on the loading, release and cytotoxicity profiles†

Andreas M. Nyström,[a] Zhiqiang Xu,[b] Jinqi Xu,[a] Sara Taylor,[b] Thalia Nittis,[c] Sheila A. Stewart,[c] Jeffrey Leonard[b] and Karen L. Wooley*[a]

Received (in Cambridge, UK) 1st April 2008, Accepted 2nd May 2008
First published as an Advance Article on the web 10th June 2008
DOI: 10.1039/b805428b

SCK nanoparticles having differing core thermal characteristics were designed and evaluated as thermoresponsive drug delivery systems of doxorubicin for the killing of cancerous cells.

Nanoobjects, such as polymeric micelles and nanoparticles, are considered to be promising vehicles for the delivery of hydrophobic or amphiphilic drugs.[1–7] Such polymeric assemblies can be prepared from amphiphilic diblock copolymers, which self assemble in aqueous solution to afford nanoscale structures with a core–shell morphology. The hydrophobic core facilitates encapsulation of the drug, while the hydrophilic shell can protect the drug from its surroundings.[1–9] It is recognized that the permeability of the shell is important to gate the uptake and release of guest molecules, and also that the incorporation of residual functionality in the shell domain of these assemblies provides a handle for the attachment of various ligands for tailored biodistribution, imaging and targeting.[5,10–12] The characteristics of the core domain are also of significance.[13,14]

In this work, we have investigated the effects of the chemical composition and thermal characteristics of the hydrophobic core polymer material for the loading and release of doxorubicin (Dox). Dox is a drug widely used in chemotherapy treatments for several types of cancer.[15] Liposome encapsulation of Dox has been shown to both reduce toxicity and improve activity, and is marketed as Doxil®.[15] Several research groups have studied Dox encapsulation within, or conjugation onto, a variety of polymeric micelles and other types of nanostructures, with promising results.[4,16–21]

Shell-crosslinked knedel-like nanoparticles (SCKs) are polymeric micelles that are crosslinked through the shell region of the particle.[22,23] In our laboratory, the crosslinking is typically performed by the amidation of poly(acrylic acid) groups in aqueous solution, and this provides stability to the nanostructure, circumventing the limitations that the CMC poses for *in vivo* applications.[10,11]

We have selected two classes of SCKs from our library of nanostructures as hosts for Dox, and evaluated a series of four SCKs with different compositions and sizes.[12,24] These SCKs were constructed from amphiphilic block copolymers of either glassy amorphous poly(acrylic acid)-*b*-poly(styrene) (PAA-*b*-PS), having a high glass transition temperature, T_g,[12] or semi-crystalline poly(acrylic acid)-*b*-poly(octadecyl acrylate-*co*-decyl acrylate) (PAA-*b*-P(ODA-*co*-DA)),[24] having a low T_g, and exhibiting melting transitions, T_m, at either well below or just above physiological temperature (Table 1 and Fig. 1). The main objective of this work was to investigate the effects of the core material on the release rate of Dox at physiological temperature and pH. Four particular SCKs were prepared to test the hypothesis that nanoparticles containing core material of higher T_g and T_m values would retain Dox to a higher extent, resulting in slower diffusion-based release rates.

Dox was incorporated into the cores of the SCKs by the addition of a stock solution of Dox suspended in CH_2Cl_2, followed by evaporation of the organic solvent.[4] The organic solvent was used to both solvate the Dox and swell the SCK core to facilitate loading. The drug–nanoparticle solution was then washed extensively with a PBS buffer in a centrifugal filter at 37 °C. By this methodology, it was possible to prepare Dox–SCK, guest–host complexes with a low variation in the incorporation percentages from batch to batch (Table 1). The loading capacities of the polystyrene core-based SCKs, **1** and **2**, were very similar (19% and 18%, respectively), and were independent of the block lengths of the polymer precursors, indicating that the loading capacity is similar in a PS amorphous core. In the case of the semi-crystalline SCKs, the SCK with the highest proportion of crystalline monomer (ODA) also had the highest loading capacity, suggesting that it forms a more stable core for the entrapment of hydrophobic drugs.

The release of the entrapped drug from the SCK nanoparticles was assessed by monitoring the decrease over time of the concentration of Dox in dialysis cassettes.[4] The dialysis was performed at 37 °C in 5 mM PBS at pH 7.4. Samples were withdrawn from the cassettes at different times and analyzed by UV-vis spectroscopy (abs @ 488 nm, ε = 12 500 M^{-1} cm^{-1}). Fig. 2 (bottom panel) depicts the release from the amorphous SCKs, **1** and **2**, and the crystalline SCKs, **3** and **4**. The behavior of the SCKs with PS cores was very similar, with a release of *ca.* 20% of the therapeutic cargo in 8 h, followed by a slow release over 48 h. It is reasonable that the release profile of SCKs **1** and **2** should be similar, given that

[a] *Center for Materials Innovation, Department of Chemistry and Department of Radiology, Washington University in Saint Louis, Saint Louis, Missouri 63130-4899, USA. E-mail: klwooley@artsci.wustl.edu; Fax: +1 314 935-9844; Tel: +1 314 935-7136*
[b] *Department of Neurological Surgery, Washington University School of Medicine, 660 S. Euclid Avenue, CB 8057, Saint Louis, Missouri 63110, USA*
[c] *Department of Cell Biology and Physiology, 660 S. Euclid Avenue, CB 8228, Washington University in Saint Louis, Saint Louis, Missouri 63110, USA*

† Electronic supplementary information (ESI) available: Synthetic details, cell images, and DSC, DLS and FACS data. See DOI: 10.1039/b805428b

Table 1 Summary of the prepared SCK–drug conjugates

Sample	Polymer	D/nm[a]	D_h/nm[b]	T_m/°C	[Dox]/μM	Loading (%)[c]
1	PAA_{60}-*b*-PS_{30}	11 ± 1	17 ± 2	—	89 ± 10	19 ± 2
2	PAA_{100}-*b*-PS_{140}	25 ± 1	34 ± 4	—	91 ± 4	18 ± 1
3	PAA_{97}-*b*-P(ODA_{69}-*co*-PDA_{23})	29 ± 6	54 ± 5	42.0	82 ± 3	18 ± 1
4	PAA_{97}-*b*-P(ODA_{24}-*co*-PDA_{64})	50 ± 6	58 ± 6	1.5	69 ± 10	14 ± 2

[a] By transmission electron microscopy. [b] By dynamic light scattering. [c] Average weight percent loading of Dox per nanoparticle mass from two loading batches. The preparation of SCKs **1–4** is described elsewhere.[12,24] The nominal crosslinking extents of the shells were 50% in each case.

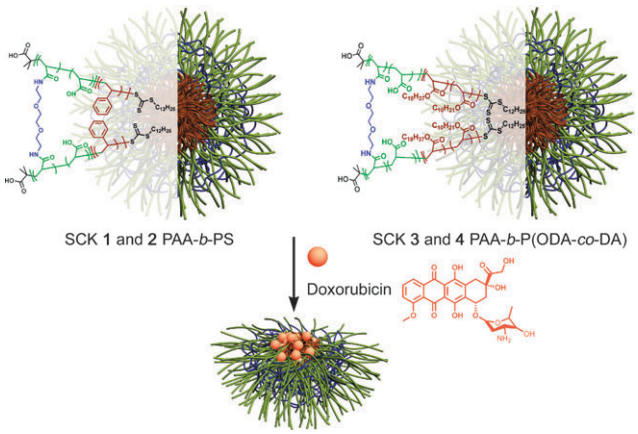

Fig. 1 Schematic representation of the SCKs prepared in the study.

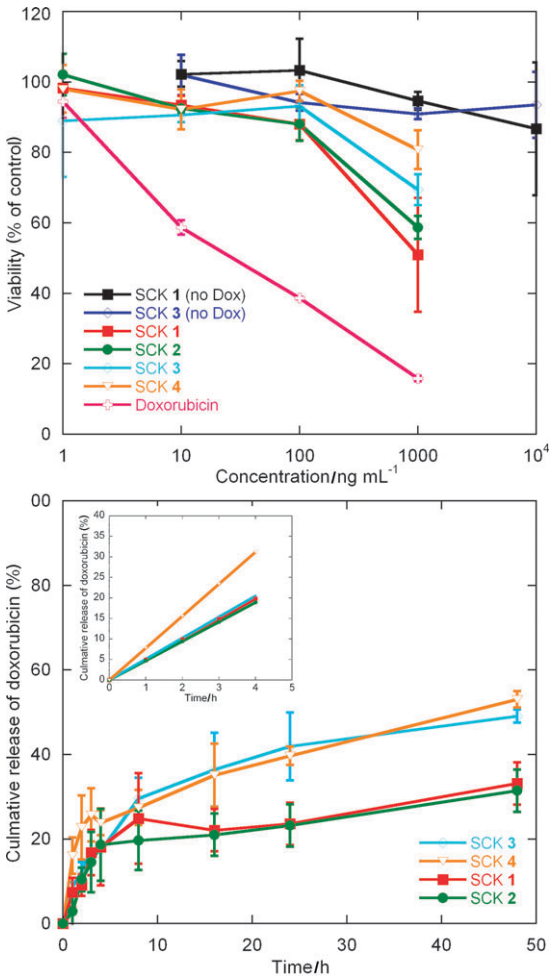

Fig. 2 Top: MTT assay of SCKs **1** and **3** without Dox loading at 72 h incubation, and MTT assay of SCKs **1–4** with Dox loading. Bottom: release kinetics of SCKs **1–4** (average of $n = 2$).

their chemical environments are the same, even though there are differences in the sizes of their amorphous cores. SCKs **1** and **2** also differ in their expected shell thicknesses, as they are derived from block copolymers of different PAA chain segment lengths; however, they have the same crosslinking density. For these nanoparticles of 10–38 nm overall diameter, it appears that the dimensions of the core and shell are not determining factors in the guest release profiles. In the case of semi-crystalline SCKs **3** and **4**, release of the cargo was slightly faster than that observed from the PS-cored SCKs, with a release of *ca.* 30% in 8 h, followed by a gradual release to *ca.* 50% after 48 h. The most significant difference can be seen in the inset of Fig. 2 (bottom panel), where the low T_m SCK, **4**, has a much faster release rate during the first 4 h compared to SCKs **1–3**. The release of therapeutics from crystalline and amorphous micelles of the same chemical composition has been shown to result in different release kinetics.[25] In order to assess whether the loading of a small molecule therapeutic could disrupt the crystallization of SCK **3**, we conducted DSC experiments on a lyophilized sample of SCK **3** containing Dox (see ESI†). SCK **3** had a T_m of 42.0 °C before guest loading, and the incorporation of Dox resulted in a reduction of melting point to 36.1 °C, which is lower than the temperature at which the release experiments were conducted. This melting point depression is advantageous; reducing the T_m to just below 37 °C provides for nanoparticles that can physically trap Dox in a crystalline matrix at room temperature and release it from a molten core at physiological temperature. The overall release extents for each of the molten-cored SCKs were greater than for the PS core, which is expected to retain a portion of Dox within its glassy core matrices.

The cytotoxicities of the non-loaded SCKs were determined by incubating U87-MG-EGFRvIII-CBR cells (a human glioblastoma cell line modified to express the mutant EGFRvIII receptor and click beetle red luciferase) with varying concentrations of SCKs **1** and **3** (Fig. 2, top panel). Cell viability was assessed using a Vybrant MTT cell proliferation assay kit. After 72 h of incubation with nanoparticles not containing Dox, no significant toxicity was observed at concentrations up to 10 μg mL^{-1}. Given that the IC_{50} of free Dox is similar (approximately 100–200 ng mL^{-1}) for both parental U87-MG[26] and U87-MG-EGFRvIII-CBR cells (Fig. 2, top panel), these nanoparticles are expected to allow for the delivery of effective doses of Dox to tumor cells, with minimal toxic effects from the SCK carriers. The cytotoxic effects of Dox loaded within and released from SCKs **1–4** were then tested on

U87-MG-EGFRvIII-CBR cells *in vitro* using the MTT assay (Fig. 2, top panel). All four Dox–SCK complexes demonstrated cytotoxic effects on U87-MG-EGFRvIII-CBR. We reasoned that the distribution, kinetics of release, and availability of Dox inside the cells between Dox–SCK complexes and free Dox are different, and that this may account for the difference in their cytotoxic effects. FACS analysis showed that the reduced viability of the cells was caused by an increase in apoptosis (see ESI†).

To investigate the cellular uptake and trafficking of Dox–SCK complexes in U87-MG-EGFRvIII-CBR cells, we performed microscopic studies based on the red auto-fluorescence from Dox. Most of the auto-fluorescence from Dox–SCK complexes was localized in the cytoplasm, specifically in the perinuclear region, while cells treated with free Dox demonstrated significant auto-fluorescence in the nucleus (see ESI†).

Red auto-fluorescence was also observed in Dox–SCK complexes that were co-localized with a fluorescent lysosome marker (lysotracker, data not shown), suggesting that these complexes were indeed endocytosed into lysosome organelles. Lysosomal trapping of Dox–SCK complexes may control the release of Dox inside the cells, thus limiting their cytotoxic effects, compared with free Dox. We are currently testing several lysosome perturbent agents combined with these Dox–SCK complexes to enhance their therapeutic efficacy on human glioma cell lines.

In this work, we have demonstrated the successful incorporation of Dox into nanoparticle vehicles for drug delivery. Release of the incorporated therapeutic agent was demonstrated in a dialysis model, and the release rate was shown to be dependent on the core material. Theoretical studies have indicated that enthalpic interactions between the core material and the drug are an important factor in governing release behavior.[14] Intermolecular interactions in combination with thermal properties could account for the reduced release of Dox in the PS-cored particles, since the core is capable of forming π–π interactions with the drug. However, the overall shapes of the release curves are similar, which suggests that the release behavior of these two classes of SCK is predominantly governed by the general nanoparticle core–shell morphology, and is less dependent on the composition of the core domain (PS *vs.* P(ODA-*co*-DA)). We have achieved excellent loading capacities, with releases extending over several hours. Burst release was avoided by the purification protocol employed. The Dox–SCK complexes were shown to kill U87-MG-EGFRvIII-CBR cancer cells and the SCKs themselves did not negatively affect the viability of these cells. These SCKs show promise as a nanoparticle platform for drug delivery. Further investigation of additional SCKs with broader core compositions and characteristics tailored for particular drugs are needed to investigate their ability to attract and retain guest molecules to differing degrees. We are currently modifying our nanoparticle carriers for targeted drug delivery by introducing poly(ethylene glycol) chains for increased *in vivo* circulation time, tags for imaging, and targeting moieties for tissue-specific binding.

This material is based upon work supported by The Children's Discovery Institute of St. Louis Children's Hospital and Washington University School of Medicine, and the National Heart, Lung, and Blood Institute of the National Institutes of Health as a Program of Excellence in Nanotechnology (HL080729). A postdoctoral and assistant professor fellowship provided by the Knut and Alice Wallenberg Foundation is gratefully acknowledged (A. M. N.).

Notes and references

1. T. M. Allen and P. R. Cullis, *Science*, 2004, **303**, 1818–1822.
2. R. Duncan, *Nat. Rev. Drug Discovery*, 2003, **2**, 347–360.
3. G. Gaucher, M.-H. Dufresne, V. P. Sant, N. Kang, D. Maysinger and J.-C. Leroux, *J. Controlled Release*, 2005, **109**, 169–188.
4. E. R. Gillies and J. M. J. Fréchet, *Bioconjugate Chem.*, 2005, **16**, 361–368.
5. K. Kataoka, A. Harada and Y. Nagasaki, *Adv. Drug Delivery Rev.*, 2001, **47**, 113–131.
6. R. Langer, *Nature*, 1998, **392**, 5–10.
7. A. Rösler, G. W. M. Vandermeulen and H.-A. Klok, *Adv. Drug Delivery Rev.*, 2001, **53**, 95–108.
8. M. Malmsten, *Soft Matter*, 2006, **2**, 760–769.
9. N. Rapoport, *Prog. Polym. Sci.*, 2007, **32**, 962–990.
10. R. K. O'Reilly, C. J. Hawker and K. L. Wooley, *Chem. Soc. Rev.*, 2006, **35**, 1068–1083.
11. E. S. Read and S. P. Armes, *Chem. Commun.*, 2007, 3021–3035.
12. G. Sun, J. Xu, A. Hagooly, R. Rossin, Z. Li, D. A. Moore, C. J. Hawker, M. J. Welch and K. L. Wooley, *Adv. Mater.*, 2007, **19**, 3157–3162.
13. J. L. Turner, Z. Chen and K. L. Wooley, *J. Controlled Release*, 2005, **109**, 189–202.
14. G. A. Buxton and N. Clarke, *Soft Matter*, 2007, **3**, 1513–1517.
15. D. D. Lasic, *Nature*, 1996, **380**, 561–562.
16. C. C. Lee, E. R. Gillies, M. E. Fox, S. J. Guillandeu, J. M. J. Fréchet, E. E. Dy and F. C. Szoka, *Proc. Natl. Acad. Sci. U. S. A.*, 2006, **103**, 16649–16654.
17. M. D. Chavanpatil, A. Khdair, B. Gerard, C. Bachmeier, D. W. Miller, M. P. V. Shekhar and J. Panyam, *Mol. Pharm.*, 2007, **4**, 730–738.
18. K. S. Soppimath, L.-H. Liu, W. Y. Seow, S.-Q. Liu, R. Powell, P. Chan and Y. Y. Yang, *Adv. Funct. Mater.*, 2007, **17**, 355–362.
19. B. Petri, A. Bootz, A. Khalansky, T. Hekmatara, R. Mueller, R. Uhl, J. Kreuter and S. Gelperina, *J. Controlled Release*, 2007, **117**, 51–58.
20. S. J. Guillaudeu, M. E. Fox, Y. M. Haidar, E. E. Dy, F. C. Szoka and J. M. J. Fréchet, *Bioconjugate Chem.*, 2008, **19**, 461–469.
21. P. A. Bertin, D. Smith and S. T. Nguyen, *Chem. Commun.*, 2005, 3793–3795.
22. K. B. Thurmond, T. Kowalewski and K. L. Wooley, *J. Am. Chem. Soc.*, 1996, **118**, 7239–7240.
23. K. B. Thurmond, T. Kowalewski and K. L. Wooley, *J. Am. Chem. Soc.*, 1997, **119**, 6656–6665.
24. A. M. Nyström and K. L. Wooley, *Soft Matter*, 2008, 849–858.
25. S. K. Agrawal, N. Sanabria-DeLong, J. M. Coburn, G. N. Tew and S. R. Bhatia, *J. Controlled Release*, 2006, **112**, 64–71.
26. X. Pan and R. J. Lee, *Int. J. Pharm.*, 2007, **336**, 276–283.